

Development and Optimization of Grain Storage Composites Using Crop Residues: A Study on Physical Performance Improvement

Deepak Kumar Mishra^{*}, B.R. Singh¹, Suresh Chandra¹, Jaivir Singh¹, Vivak Baliyan¹, Neelesh Chauhan¹

¹- College of Technology, Sardar Vallabhbhai Patel University of Agriculture and Technology, Meerut-250110

^{*} Corresponding author

Email: Deepakmishrasvp@gmail.com

ARTICLE INFO	ABSTRACT
Received: 30 Dec 2024	<p>This study explores the development of sustainable agro-composite materials for enhancing grain storage, particularly in resource-limited areas. The composites, made from agricultural residues such as bagasse, wood sawdust, paddy straw, and mustard husk, were reinforced with epoxy resin and silica fillers. Thirty-six samples were prepared by varying the residue and epoxy resin content, while maintaining constant amounts of silica and hardener. The composites were evaluated for physical properties including water absorption, dry density, and dimensional stability. Among the samples, the T32 composite, consisting of 600 g wood sawdust, 100 g silica, and 100 ml hardener, showed promising results at a cost of ₹25.2 per kg, lower than steel bins. A strong correlation between the residue-epoxy ratio and weight density was observed in paddy straw composites, yielding high R^2 and adjusted R^2 values. Uncertainty analysis was also performed to assess the accuracy of the research. This study demonstrates the potential of agro-waste composites as cost-effective, biodegradable, and sustainable alternatives for grain storage, aligning with circular economy principles.</p> <p>Keywords: Agro-composites, Agricultural Waste, Grain Storage, Post-Harvest Losses, Sustainable Materials.</p>
Revised: 12 Feb 2025	
Accepted: 26 Feb 2025	

Nomenclature

English Letter Symbols

A	:	Surface area of sample [m^2]
L	:	Length of sample [mm]
W	:	Width of Sample [mm]
T	:	Thickness of Sample [mm]
h	:	Thickness of composite panel
m	:	Mass of composite sample [g]
W	:	Weight [g.cm/ Sec^2]
V	:	Volume of composite sample [cm^3]
ρ	:	Density [g/cm^3 or kg/m^3]
A	:	Weight Density of Paddy Straw composite sample [$\text{g}/\text{sec}^2.\text{cm}^2$]
B	:	Weight Density of Bagasse composite sample [$\text{g}/\text{sec}^2.\text{cm}^2$]
C	:	Weight Density of Mustard Stalk composite sample [$\text{g}/\text{sec}^2.\text{cm}^2$]
D	:	Weight Density of Wood Sawdust composite sample [$\text{g}/\text{sec}^2.\text{cm}^2$]
P_{cum}	:	Cumulative Percentage
RER	:	Residue-Epoxy Ratio

Greek Letter Symbols

δ	:	Absolute uncertainty
Δ	:	Change

Subscripts

- 1,i : Initial condition
2,f : Final condition

Abbreviations

- MS : Mean Square
SS : Sum of Square
df : Degree of Freedom
WA : Water Absorption
TS : Thickness swelling percentage
T : Test Sample

1. Introduction

The increasing global emphasis on sustainability within agriculture and materials science has accelerated the development of biodegradable and eco-conscious alternatives to conventional construction and packaging materials. In the context of grain storage, particularly in rural and low-income areas, there is an overdependence on conventional resources such as steel, cement, and synthetic polymers. These materials not only contribute to environmental degradation due to their carbon-intensive manufacturing processes but also impose significant economic burdens due to their non-renewable nature and limited recyclability [1].

Agricultural byproducts like bagasse, paddy straw, sawdust, and mustard husk are produced in substantial volumes in agrarian regions and are often incinerated, which exacerbates air pollution and greenhouse gas emissions [2]. However, these residues possess valuable properties that make them suitable reinforcements in composite materials. When integrated with epoxy resin and silica fillers, they can yield mechanically robust, moisture-resistant, and dimensionally stable panels ideal for grain storage applications [3].

2. Literature Review

2.1 Review of Existing Grain Storage Technologies

Grain preservation post-harvest is highly sensitive to environmental conditions including temperature, humidity, pH, and oxygen levels. These factors play a vital role in determining the physico-chemical integrity of stored grains. Sashidhar et al. emphasized that fluctuations in temperature and humidity can accelerate biological degradation and enzymatic reactions, ultimately reducing shelf life and nutritional quality [4]. Furthermore, inadequate storage environments promote infestations by weevils, beetles, moths, and rodents, contributing to significant post-harvest losses [5]. In developing economies, approximately 60–70% of grains are stored at the household level in traditional facilities, with decisions on storage practices largely influenced by socio-economic variables such as landholding size, market trends, credit access, and consumption needs [6].

Traditional storage systems are built from accessible materials like bamboo, straw, cow dung, mud, and wood, reflecting region-specific architectural practices. These structures—often cylindrical, spherical, or cuboidal—may be situated indoors or underground to enhance insulation and passive cooling [7], [8]. Despite their low cost and cultural acceptance, they lack standardized designs and are poorly equipped to regulate humidity or prevent pest and fungal intrusion. Their efficacy is largely climate-dependent, and they often deteriorate rapidly in humid or termite-prone regions [9].

Modern storage systems like concrete, galvanized steel, and wooden silos offer improved durability and environmental control. Concrete silos are particularly valued in coastal areas for their resistance to corrosion, though they require steel reinforcement due to concrete's low tensile strength [10]. Double-walled designs with air gaps mitigate internal condensation, thereby preserving grain quality. Wooden silos provide better thermal insulation but are highly vulnerable to termites, with damage often remaining undetected until structural compromise occurs [11].

Emerging alternatives include silos made from termite mound clay (TMC), which offer enhanced thermal stability and moisture control. These materials naturally resist fungal growth and thermal gradients, making them suitable for low-cost tropical applications [12]. In comparative studies, galvanized steel silos showed the best long-term

performance in maintaining optimal moisture levels and preventing humidity ingress, followed by reinforced concrete and TMC variants [13].

Hermetic storage has gained popularity for its oxygen-limiting, pest-resistant design. Purdue Improved Crop Storage (PICS) bags eliminate the need for chemical fumigants, thereby promoting safer and more sustainable grain preservation [14]. Similar innovations like hermetic bins for minor millets (developed by ICRISAT) ensure prolonged shelf life and protection from infestation under ambient conditions [15]. These solutions are especially useful in rural or marginal farming systems where refrigeration or pest control infrastructure is unavailable [16].

There is growing interest in utilizing agricultural residues such as rice husk, jute fiber, coir, and coconut pith for creating eco-friendly structural materials. These agro-wastes are renewable, biodegradable, and cost-effective, offering viable alternatives to synthetic composites [17]. Natural fiber-reinforced polymer composites—especially epoxy-based systems—combine high mechanical strength with environmental compatibility. Epoxy resins are preferred for their strong adhesion, thermal stability, and resistance to environmental degradation [18].

Fillers like silica and calcium carbonate are used to enhance composite properties such as tensile and impact strength. Studies show that nano-silica fillers can improve dispersion and interfacial bonding in epoxy matrices, leading to enhanced toughness and thermal conductivity even at filler loadings below 10% by weight [19]–[21].

Research into natural fiber composites has yielded promising results. Osarenmwinda et al. developed predictive models for mechanical properties of sawdust-epoxy and palm kernel shell composites, achieving deviations below 10% between experimental and theoretical values [22]. Junjun et al. enhanced rice straw composite strength through alkali pretreatment and starch-based adhesives, improving flexural strength by over 30% [23]. Hot water treatment was found by Liu et al. to increase fiber adhesion and moisture resistance in straw-reinforced boards [24].

Verma et al. explored bamboo fiber laminates with epoxy matrices, reporting excellent tensile and flexural performance, indicating suitability for both structural and packaging applications [25]. Manji et al. found that increasing rice straw content in polypropylene composites improved both modulus and strength, offering a sustainable alternative to petroleum-based plastics [26]. Dsouza et al. applied bio-composites to yak saddles in high-altitude regions, achieving 30% higher load capacity and reduced costs compared to traditional wooden designs [27].

To address regional climatic challenges, customized silo designs have been proposed. Adejumo engineered a double-walled, 350 kg capacity metallic silo with improved airflow and moisture regulation features tailored for tropical use [28]. Bhardwaj highlighted the effectiveness of Pusa bins in high-humidity climates due to their vapour-tight walls [29]. Similarly, Hapur and Coal Tar Drum bins have demonstrated portability and corrosion resistance, making them ideal for smallholder farmers in diverse agro-climatic zones.

While traditional systems remain dominant due to affordability and familiarity, they offer limited protection against biotic and abiotic stressors. Modern and hermetic systems, although effective, are often cost-prohibitive or logistically complex. The future of grain storage lies in scalable, regionally adaptable solutions that integrate bio-composites and passive climatic control features. Further research is required to validate long-term performance of these systems under diverse climatic conditions and to optimize composite formulations for durability, affordability, and biodegradability. This investigation centers on the formulation of composite grain storage panels using various proportions of agricultural residues, while maintaining fixed quantities of epoxy binder and silica fillers. A total of twelve formulations were developed, varying the biomass input (500 g, 600 g, and 700 g), with constant amounts of silica (100 g) and hardener (100 ml). The physical characteristics of each composite, including water absorption, dry density, and dimensional stability (shrinkage and swelling), were evaluated using standardized protocols from IS: 2380 (Parts 3 and 16) [30].

2.2 Research Gap based on above Literature Review

Despite the growing body of research on agro-waste-based composites in construction and packaging, their specialized application in grain storage has not been adequately explored. Existing literature largely focuses on generic applications like insulation and panel boards, overlooking the specific performance requirements particularly moisture resistance needed for grain storage.

Another limitation is the lack of integration of biodegradability and recycling metrics in material development, which are essential for supporting circular economy models. Moreover, many studies fail to adhere to standardized testing methodologies especially those aligned with Indian Standards hindering practical deployment in domestic markets. Addressing these gaps is critical for developing sustainable, cost-effective grain storage solutions that utilize locally available agricultural waste while complying with national quality benchmarks.

2.3 Novelty of the Present Study

This study presents a novel approach to developing eco-friendly composite materials for grain storage by utilizing biodegradable agro-resources such as bagasse, sawdust, paddy straw, and mustard husk, reinforced with epoxy resin and silica filler. Aimed at replacing traditional and metal storage structures, the research evaluates key physical properties including moisture absorption, dry density, and dimensional stability of various composite formulations. Standardized testing was conducted in accordance with IS: 2380 (Part 3 and Part 16) - 1977. Following the physical assessments, a cost analysis will be carried out to identify the most economical composite among the tested materials. The results underscore the potential of these composites as sustainable and cost-effective solutions for grain storage in rural and resource-constrained regions, distinguishing this work as a novel contribution compared to existing studies.

2.4 Applications in Various Fields

The implications of this research span multiple sectors. In agriculture and rural development, these panels offer a sustainable replacement for conventional plastic or metal silos, promoting eco-friendly grain storage while supporting farmer incomes. In the packaging industry, the composites can be utilized for biodegradable and water-resistant packaging of dry commodities, seeds, and animal feed, providing an alternative to single-use plastics [32].

In construction and civil engineering, these composites may serve as partition boards or thermal insulation materials for green buildings and temporary shelters. From an environmental standpoint, valorizing crop residues in this way helps reduce open burning, thereby lowering pollution levels [2]. Additionally, the lightweight and portable nature of the panels makes them suitable for emergency and disaster-relief grain storage, especially in flood- or drought-affected regions.

3. Materials and Methods

3.1 Selection of Crop Residues for Agro-Composite Development

Agro-composites are developed by selecting filler materials that improve mechanical strength, thermal stability, and biodegradability. Crop residues like paddy straw, bagasse, mustard stalk, and wood sawdust are ideal due to their fibrous nature, abundance, and low cost. These bio-based fibers, when combined with matrices such as epoxy resin and fillers like silica, enhance composite performance. This approach not only strengthens the material but also promotes sustainability by utilizing agricultural waste, making it a cost-effective and eco-friendly choice for composite production.

3.1.1 Epoxy Resin as a Reinforcing Filler in Agro-Composite Development

Epoxy resins are widely utilized in diverse industrial sectors due to their superior mechanical strength, excellent adhesion to various substrates, and remarkable resistance to thermal and chemical degradation [33]. A notable commercial example is Araldite CY-230, a low-viscosity, solvent-free epoxy resin based on bisphenol-A, extensively used in structural bonding, coatings, and electrical insulation. The resin cures effectively under ambient conditions (20–25°C and atmospheric pressure) when mixed with a compatible hardener such as Hardener HY-951, which contains aliphatic amine components. The curing reaction converts the resin into a highly cross-linked, rigid thermoset polymer exhibiting exceptional strength and dimensional stability. Key mechanical and electrical properties of the cured Araldite CY-230 system are summarized in Table 1.

Table 1: Typical Properties of Cured Araldite CY-230 / Hardener HY-951 System

S. No.	Property	Value
1	Tensile Strength [34]	75–85 MPa
2	Flexural Strength [34]	100–120 MPa
3	Young's Modulus [34]	2.5–3.0 GPa
4	Hardness (Shore D) [34]	85–90
5	Dielectric Strength [35]	>18 kV/mm
6	Volume Resistivity [35]	>10 ¹⁴ ohm-cm
7	Dielectric Constant (1 MHz) [35]	3.2–3.5
8	Operating Temperature Range [36]	–40°C to +120°C
9	Short-Term Thermal Endurance [36]	Up to 150°C
10	Coefficient of Linear Thermal Expansion [36]	50–60 ppm/°C

The resin system exhibits excellent chemical resistance to water, acids, alkalis, and various organic solvents, maintaining structural and electrical integrity across a wide temperature range. Its thermal stability and low coefficient of linear thermal expansion (CLTE) make it ideal for applications involving thermal cycling.

The resin-to-hardener ratio plays a crucial role in determining the final properties of the cured system. Based on experimental studies, an optimal hardener concentration of 9% by volume or weight results in maximum elongation, yield strength, and modulus of elasticity [37]. Inadequate hardener content (<8%) can lead to incomplete curing and a tacky surface, while excess hardener (>9%) may cause uncontrolled exothermic reactions, risking thermal degradation of the matrix [37]. Thus, a 9% v/v ratio is recommended to achieve a balanced cross-linking density, ensuring optimal mechanical performance, durability, and thermal resistance in composite applications.

3.1.2 Silica as a Reinforcing Filler in Agro-Composite Development

Silica (SiO₂) is a widely used inorganic filler in polymer matrix composites due to its excellent mechanical reinforcement capabilities, thermal stability, and wear resistance properties. The inclusion of silica particles, particularly those with uniform spherical morphology, has been shown to significantly reduce the wear rate of epoxy-based composites by improving interfacial bonding and enhancing load-bearing capacity. Research has demonstrated that incorporating silica particles with diameters in the nanoscale range—specifically around 120 nm and 510 nm—leads to improved abrasion resistance and surface hardness when compared to unfilled epoxy systems [38].

According to experimental studies, an optimal silica content between 5.0 wt% and 10.0 wt% results in maximum improvement in mechanical and tribological behavior, with diminishing returns beyond this range due to particle agglomeration and poor dispersion [39]. In the present study, silica with a mesh size of 60 to 120 (corresponding to a particle size of approximately 125–250 μ m) is selected to balance dispersion, surface interaction, and cost-effectiveness. A concentration of 10.0 wt% silica is employed to ensure optimal reinforcement without compromising the matrix integrity or inducing processing challenges. The selected silica contributes to enhanced stiffness, reduced coefficient of friction, and improved resistance to surface wear, making it a suitable filler for structural and biodegradable agro-composite applications. Table 2 presents the key physical and chemical properties of silica utilized as a reinforcing filler in the composite development

Table 2: Properties of Silica Used in Composite Development

S. No.	Property	Value/Range
1	Chemical formula	SiO ₂
2	Particle shape [38]	Spherical
3	Particle size (nano) [38]	120 nm / 510 nm (nano-scale)
4	Particle size (mesh)	60–120 mesh (~125–250 μ m)
5	Purity [40]	>99%
6	Specific gravity [40]	~2.65

7	Hardness (Mohs scale) [40]	~7
8	Dielectric constant [40]	3.9–4.2
9	Thermal conductivity [40]	~1.4 W/m·K
10	Optimal concentration in epoxy [39]	5.0–10.0 wt%
11	Selected concentration for study	10.0 wt%

3.1.3 Agro-degradable Reinforcing Materials in Composite Development

Reinforcing agents are essential for enhancing the mechanical strength, wear resistance, and overall performance of composite materials. In this study, various agro-degradable materials — paddy straw, bagasse, mustard stalk, and wood sawdust — were utilized as reinforcing agents within resin matrices to improve the properties of the resulting composites. These agro-residues were chosen for their fibrous structure, abundance, and biodegradability, making them highly suitable for sustainable composite fabrication. The integration of these bio-based materials with epoxy resin matrices and silica fillers contributed to improved mechanical performance and thermal stability.

According to Singh et al. [40], optimal results were obtained when bio-waste materials were mixed in equal proportions (by weight) with silica particles sized between 60 and 120 mesh. This combination significantly enhanced the composite's mechanical strength, wear resistance, and overall durability. Based on these findings, a 1:1:1 ratio of bio-waste, silica, and matrix material was identified as optimal for developing biodegradable composites. Further, the study examined the effects of varying bio-waste content, selecting 5%, 10%, and 15% weight percentages to assess their impact on the composites' overall properties. The bio-degradable materials not only provide structural reinforcement but also enhance the environmental sustainability of the composites by utilizing agricultural waste. The addition of agro-degradable fillers results in composites that exhibit improved mechanical properties while being more eco-friendly and biodegradable compared to traditional synthetic composite materials. Table 3 summarizes the properties of different agro-degradable materials used as reinforcing agents.

Table 3: Properties of Agro-Degradable Materials Used as Reinforcing Agents

S. No.	Material	Fiber Content (%)	Mechanical Properties	Biodegradability	Potential Applications
1	Paddy Straw	30-40%	High tensile strength, moderate stiffness	High	Structural composites
2	Bagasse	45-55%	Moderate stiffness, impact resistance	Moderate	Biodegradable packaging
3	Mustard Stalk	35-45%	Low flexibility, low wear resistance	High	Eco-friendly composites
4	Wood Sawdust	50-60%	High wear resistance, moderate strength	High	Biodegradable boards

These materials, combined with epoxy resin and silica fillers, offer a range of benefits such as improved mechanical properties, biodegradability, and enhanced performance in composite structures.

3.2 Fabrication Methodology of Agro-Residue-Based Epoxy Composites

To develop eco-friendly polymer composites, a systematic casting process was adopted using various agro-based residues—namely, paddy straw, bagasse, mustard stalk, and wood sawdust—as reinforcing fillers. The matrix material used was a thermosetting epoxy resin (LY-556), while silica (mesh size: 60–120) served as a secondary filler to enhance the mechanical and thermal properties of the composite. A total of 36 unique composite shown in figure 1, formulations were prepared by varying the proportion of agricultural residues from 500 g to 700 g in increments of 25 g. The quantity of silica (100 g) and the curing agent, i.e., hardener HY-951 (100 ml), were kept constant across all samples to maintain consistency in matrix reinforcement behavior.

3.2.1 Processing Procedure

The process began by weighing the required quantities of agro-residue and silica, which were then thoroughly blended. The epoxy resin was heated in an electric furnace to 75°C for 20 minutes, operating within a temperature range of 0°C to 300°C. After the heating cycle, the resin mixture was allowed to cool naturally to around 45°C. At this point, 100 ml of hardener (HY-951) was added and mixed thoroughly to form a highly viscous and reactive mixture. This resin-hardener mixture was then combined with the agro-residue and silica blend and mixed thoroughly. The resulting mixture was cast into pre-cleaned molds using the hand lay-up technique. The molds were left to cure at ambient conditions for 24 hours.

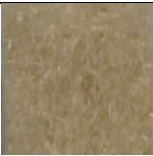

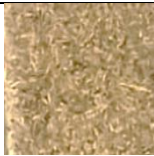

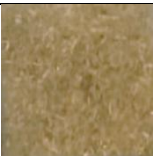
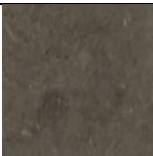

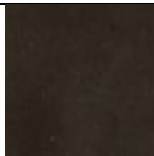



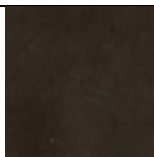





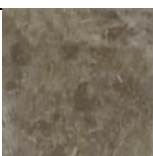



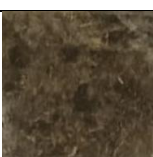




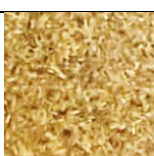
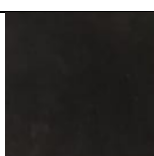
3.2.2 Composite Formulation Table

The specific compositions of the 36 developed composite samples are detailed in Table 4, categorized by the type of agro-residue used and the varying filler content.

Table 4: Formulations of Agro-Residue-Based Epoxy Composites

S. No.	Treatment ID	Agro-Residue Type	Residue Weight (g)	Silica (g)	Hardener (ml)	Epoxy Resin (ml)
1	T1	Paddy Straw	700	100	100	300
2	T2	Paddy Straw	675	100	100	325
3	T3	Paddy Straw	650	100	100	350
4	T4	Paddy Straw	625	100	100	375
5	T5	Paddy Straw	600	100	100	400
6	T6	Paddy Straw	575	100	100	425
7	T7	Paddy Straw	550	100	100	450
8	T8	Paddy Straw	525	100	100	475
9	T9	Paddy Straw	500	100	100	500
10	T10	Bagasse	700	100	100	300
11	T11	Bagasse	675	100	100	325
12	T12	Bagasse	650	100	100	350
13	T13	Bagasse	625	100	100	375
14	T14	Bagasse	600	100	100	400
15	T15	Bagasse	575	100	100	425
16	T16	Bagasse	550	100	100	450
17	T17	Bagasse	525	100	100	475
18	T18	Bagasse	500	100	100	500
19	T19	Mustard Stalk	700	100	100	300
20	T20	Mustard Stalk	675	100	100	325
21	T21	Mustard Stalk	650	100	100	350
22	T22	Mustard Stalk	625	100	100	375
23	T23	Mustard Stalk	600	100	100	400
24	T24	Mustard Stalk	575	100	100	425
25	T25	Mustard Stalk	550	100	100	450
26	T26	Mustard Stalk	525	100	100	475
27	T27	Mustard Stalk	500	100	100	500
28	T28	Wood Sawdust	700	100	100	300
29	T29	Wood Sawdust	675	100	100	325
30	T30	Wood Sawdust	650	100	100	350
31	T31	Wood Sawdust	625	100	100	375
32	T32	Wood Sawdust	600	100	100	400
33	T33	Wood Sawdust	575	100	100	425
34	T34	Wood Sawdust	550	100	100	450
35	T35	Wood Sawdust	525	100	100	475
36	T36	Wood Sawdust	500	100	100	500

This diverse range of composite formulations provides a robust foundation for evaluating the influence of agro-residue type and filler loading on the physical, mechanical, and thermal performance of the developed bio-composites.

Paddy Straw	Bagasse	Mustard Stalk	Wood Sawdust
			
Sample T1	Sample T10	Sample T19	Sample T28
			
Sample T2	Sample T11	Sample T20	Sample T29
			
Sample T3	Sample T12	Sample T21	Sample T30
			
Sample T4	Sample T13	Sample T22	Sample T31
			
Sample T5	Sample T14	Sample T23	Sample T32
			
Sample T6	Sample T15	Sample T24	Sample T33
			
Sample T7	Sample T16	Sample T25	Sample T34

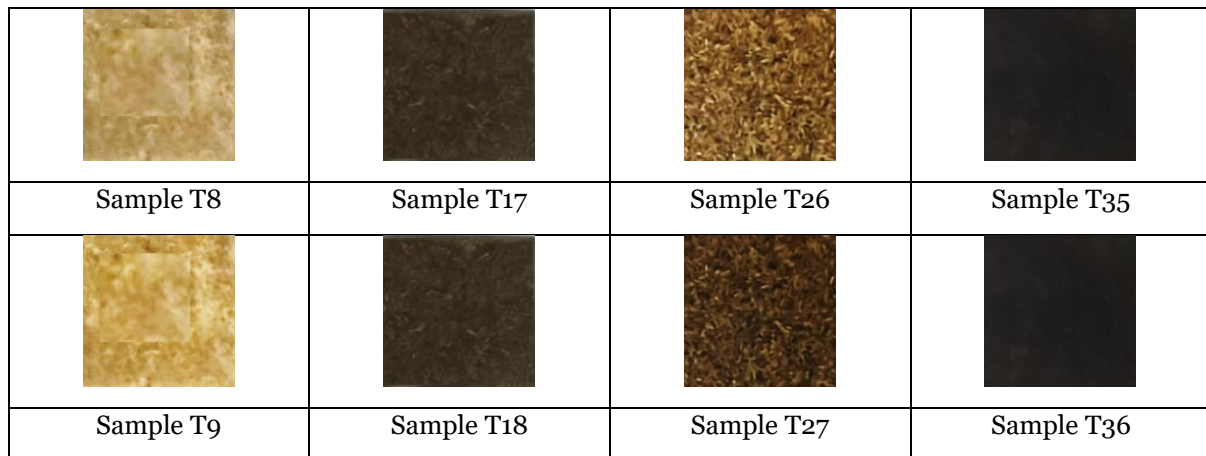


Figure 1: Image showing all 36 composite samples developed from various natural residues: Paddy Straw, Bagasse, Mustard Stalk, and Wood Sawdust.

4. Methodology for Testing and Analyzing Bio-Composite Properties

The methodology for testing and analyzing the 36 bio-composite samples focused on evaluating key physical properties. Measurements were taken at regular intervals using precise instruments.

4.1 Physical Properties

The testing procedure for the 36 bio-composite samples involved measuring density, water absorption, and thickness swelling.

4.1.1 Weight density Measurement

The weight density of the bio-composite specimens was determined using the water displacement method, a reliable technique for irregular solids. Each bio-composite sample was initially weighed using a high-precision electronic balance (least count: 0.01 g). Following this, the specimen was gently immersed in 50 mL of distilled water placed in a 100 mL graduated cylindrical beaker. The rise in water volume due to displacement was recorded to calculate the volume of the specimen.

The weight density (ρ) of the bio-composite sample was calculated using Equation (4.1):

$$\rho = \frac{W}{V} \quad \dots (4.1)$$

Where:

ρ = Weight density of the sample (g/cm³)

W = Weight of the sample (N)

V = Volume of water displaced by the sample (cm³)

This physical property is critical for evaluating the performance of bio-composite materials in structural and thermal applications. Additionally, the theoretical weight density of the composite material can be calculated based on the weight fractions and densities of individual constituents using the rule of mixtures [41], as mentioned in equation (4.2):

$$\rho_c = \left(\sum_{i=1}^n \frac{w_i}{\rho_i} \right)^{-1} \quad \dots (4.2)$$

Where:

ρ_c = Theoretical composite density

w_i = Weight fraction of the i^{th} constituent

ρ_i = Weight density of the i^{th} constituent

4.1.2 Water Absorption

Water absorption properties of the composites were evaluated as per the IS: 2380 (Part 13) – 1977 standard. Prior to testing, specimens were oven-dried at 105°C for 24 hours to remove residual moisture [42]. The dried specimens were then immersed in water maintained at a neutral pH of 7.1 and room temperature (~25°C).

The water absorption (%) at various time intervals was calculated using Equation (4.3):

$$WA(\%) = \frac{W_2 - W_1}{W_1} \times 100 \quad \dots (4.3)$$

Where: W_1 = Initial weight of the specimen (g)

W_2 = Weight after N hours of immersion (g)

4.1.3 Thickness Swelling

Thickness swelling of the 36 bio-composite samples was evaluated in accordance with IS: 2380 (Part 14) – 1977, which outlines the procedure for determining the dimensional stability of wood-based panel products under moisture exposure. The initial and post-immersion thickness of each sample was measured using Vernier calipers with a least count of 0.05 mm, and the percentage thickness swelling (TS%) was calculated using Equation (4.4):

$$TS(\%) = \frac{T_2 - T_1}{T_1} \times 100 \quad \dots (4.4)$$

Where: T_1 = Initial thickness of the specimen (mm)

T_2 = Thickness after N hours of immersion (mm)

Measurements were recorded after the samples were submerged in clean, fresh water for 2 hours. The thickness of each sample was measured using Vernier calipers with a least count of 0.05 mm, while the weight was measured using an electronic balance with a least count of 0.01 g, ensuring precision and accuracy in the evaluation.

4.2 Sieve Analysis

Sieve analysis is a widely used technique to determine the particle size distribution of granular materials, which is crucial in applications such as composite material formulation. The procedure involves passing a sample through a series of standardized sieves with different mesh sizes, and the amount of material retained on each sieve is measured to assess the particle size distribution. The mass of material retained on each sieve is expressed as a percentage of the total sample mass, which is used to construct a particle size distribution curve. The weight percentage retained on each sieve (W_i) is calculated using the equation (4.8):

$$W_i = \left(\frac{M_i}{M_{\text{total}}} \right) \times 100 \quad \dots (4.5)$$

Where: W_i is the weight percentage retained on sieve i ,

M_i is the mass of material retained on sieve i ,

M_{total} is the total mass of the sample.

The cumulative percentage passing through each sieve is then calculated to generate the particle size distribution curve. For each sieve, the cumulative passing percentage P_{cum} is given by equation (4.9):

$$P_{\text{cum}} = 100 - \sum_{i=1}^n W_i \quad \dots (4.6)$$

Where 'n' is the number of sieves. This analysis helps in determining the particle size range for various sample, which is critical for understanding the material's flow ability, compaction behaviour, and its potential use in composite formulations [44]. Sieve analysis results for materials such as paddy straw, bagasse, mustard, and wood sawdust are

typically represented as particle size distribution curves. These curves visually depict the proportion of different particle sizes within the materials, as discussed in the results section. Sieve analysis plays a vital role in ensuring that the agro-residues and fillers used in composite materials have optimal characteristics, thus contributing to the consistent and reliable performance of the composites across various applications.

5. Results and Discussions

This section discusses the physical properties of the 36 bio-composite samples, including density, water absorption, and thickness swelling, to evaluate the influence of agro-residue type and filler ratios. The results showed variations in these properties based on the agro-residue type (paddy straw, bagasse, mustard stalk, wood sawdust) and filler composition (hardener and silica content). Statistical analysis, including correlation and uncertainty, confirmed that both the agro-residue type and filler ratio significantly impacted the composite properties. Additionally, sieve analysis of the raw materials was conducted to determine their particle size distribution, which ensured the optimal selection of materials for achieving the desired performance in the composites.

5.1 Results of Sieve Analysis for various Composite

Sieve analysis was performed on 36 composite materials to examine the particle size distribution and fineness of four agricultural residues: Paddy Straw, Bagasse, Mustard Stalk, and Wood Sawdust. Each sample weighed 50 grams and was subjected to a 15-minute sieving process. The results, as depicted in Figures 5.1 to 5.4, reveal the variation in particle size and help determine the fineness of each sample according to the sieve sizes used.

For Paddy Straw (Figure 5.1), the highest percentage of material (33.77%) was retained on the 4.75 mm sieve, which made up the cumulative retention. As the sieve size decreased, the retained material on each sieve reduced, with only 2.454% of the material left in the pan. This indicates that 66.23% of the particles were smaller than 4.75 mm.

In the case of Bagasse (Figure 5.2), just 0.266% of the material was retained on the 4.75 mm sieve, signifying that the majority of particles were smaller in size. The finer particles were more prevalent in the lower sieve sizes, with 99.734% of the material passing through the 4.75 mm sieve.

For Wood Sawdust (Figure 5.3), 96.13% of the material passed through the 4.75 mm sieve, leaving only 3.87% retained. As the sieve size decreased, this trend continued, showing that Wood Sawdust mainly consists of finer particles. The pan retained 23.84% of the total material, with only 3.87% being coarser than 4.75 mm.

Similarly, for Mustard Stalk (Figure 5.4), 0.87% of the material was retained on the 4.75 mm sieve, with 99.13% of the particles passing through. As with the other materials, the finer particles were prevalent in the lower sieves, and only 1.651% of the material remained on the pan, confirming that Mustard Stalk is mostly composed of fine particles. These findings highlight the varying levels of coarseness and fineness across the four agricultural residues, providing valuable data on their particle size distribution for further processing or application.

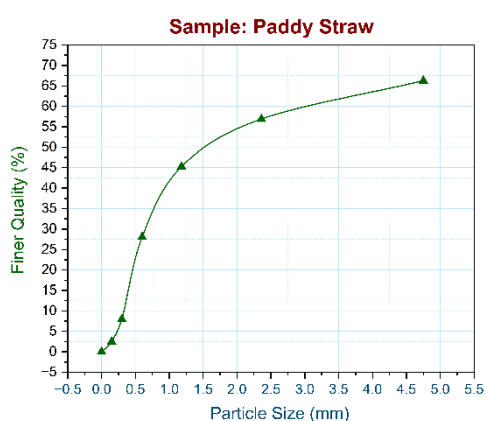


Figure 5.1: Particle size distribution of paddy straw

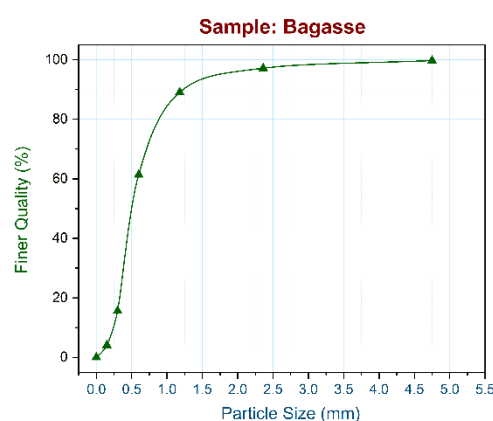


Figure 5.2: Particle size distribution of Bagasse

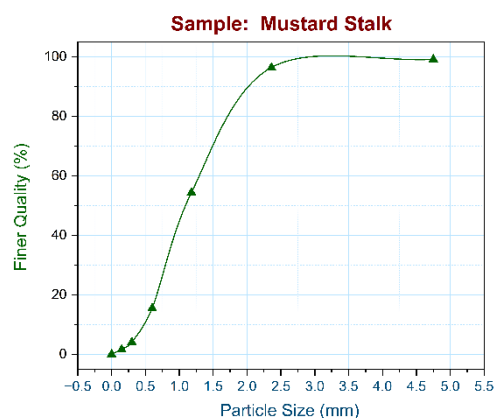


Figure 5.3 Particle size distribution of Mustard Stalk



Figure 5.4: Particle size distribution of Wood Sawdust

5.2 Results of Water Absorption Test for various Composite

The water absorption test was performed on various agro-residue composites, including Paddy Straw, Bagasse, Mustard Stalk, and Wood Sawdust, combined with silica, hardener, and resin. The results revealed distinct water absorption patterns across the different samples. For Paddy Straw (T1-T9), as shown in figure 5.5, water absorption decreased with increasing agro-residue content. At 500 grams, the absorption was 24.74%, dropping to 15.23% at 700 grams, likely due to the higher concentration of binding agents, which reduced porosity. Bagasse (T10-T18), shown in figure 5.6, exhibited significantly higher water absorption values, starting at 69.77% at 500 grams and decreasing to 9.29% at 700 grams. Its fibrous structure contributed to higher moisture retention compared to Paddy Straw. Mustard Stalk (T19-T27), shown in figure 5.7, exhibited water absorption values ranging from 35.92% at 500 grams to 6.46% at 700 grams, indicating significant, but lower, water retention than Bagasse, likely due to differences in its composition and structure. Wood Sawdust (T28-T36), shown in figure 5.8, demonstrated the lowest water absorption, starting at 45.91% at 500 grams and decreasing to 3.73% at 700 grams. The low water absorption is attributed to its reduced porosity, with the T32 sample at 600 grams showing only 3.23% absorption. This suggests that Wood Sawdust has limited water retention capacity at higher residue content, making it ideal for applications requiring low moisture retention.

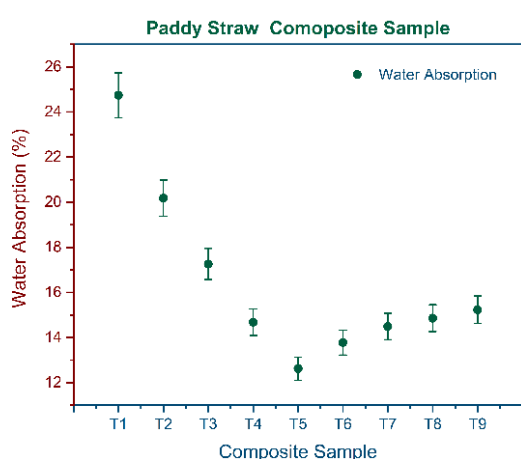


Figure 5.5: Percentage water absorption of Paddy Straw composite material

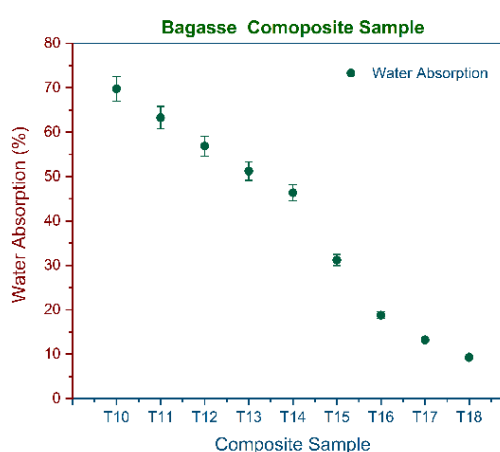


Figure 5.6: Percentage water absorption of Bagasse composite material

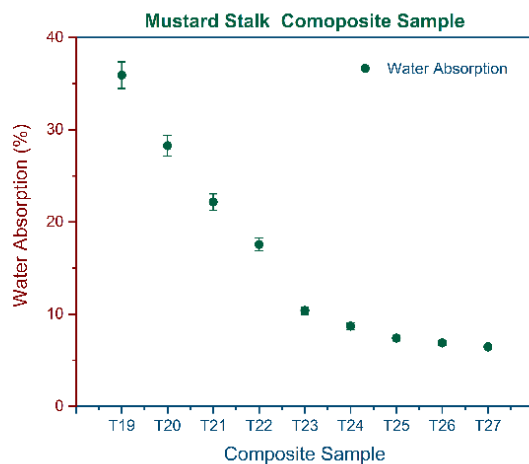


Figure 5.7 Percentage water absorption of Mustard Stalk composite material

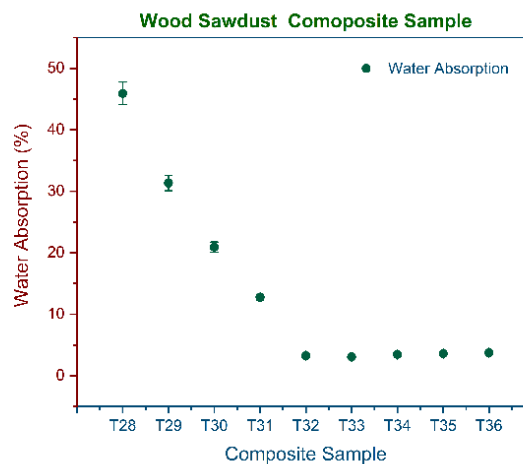


Figure 5.8: Percentage water absorption of Wood Sawdust composite material

5.3 Results of Swelling Thickness for various Composite

The swelling thickness of agro-residue composites was assessed across various treatments, showing distinct changes in thickness with varying residue content. For Paddy Straw, as shown in figure 5.9, the swelling thickness slightly increased, with a maximum change of 0.81% at 700 grams. In contrast, Bagasse, illustrated in figure 5.10, demonstrated a more substantial swelling, reaching a peak increase of 5.01% at 700 grams. Mustard Stalk, depicted in figure 5.11, displayed moderate swelling, with the highest increase of 3.33% at 700 grams. Wood Sawdust, shown in figure 5.12, exhibited the lowest swelling thickness, with a maximum change of 3.82% at 700 grams. Notably, the T32 sample of Wood Sawdust, with 600 grams of residue, showed the smallest swelling increase of just 1.53%, suggesting that higher residue content reduces swelling. These findings indicate that while all agro-residue composites experienced swelling, fibrous materials like Bagasse exhibited more pronounced changes, whereas denser materials like Wood Sawdust showed minimal swelling, especially at higher residue concentrations.

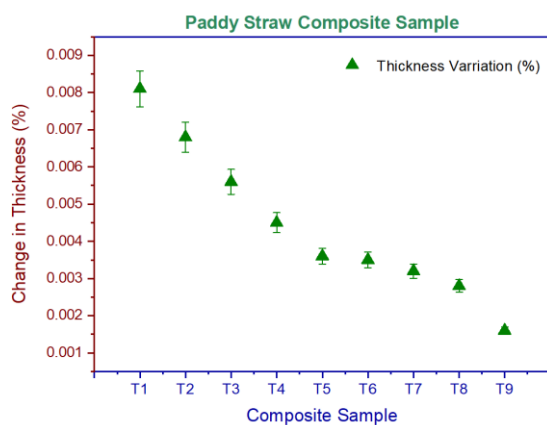


Figure 5.9: Effect of water absorption on swelling for Paddy Straw composite material

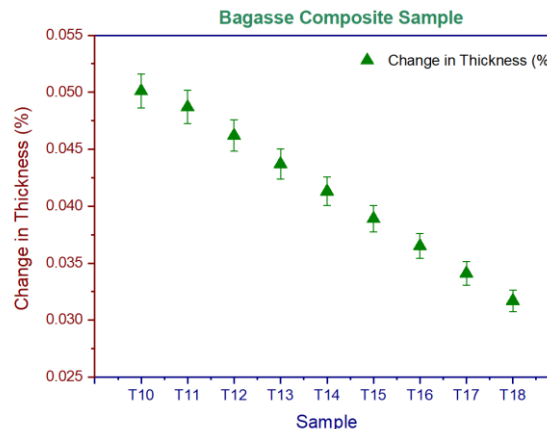


Figure 5.10: Effect of water absorption on swelling for Bagasse composite material

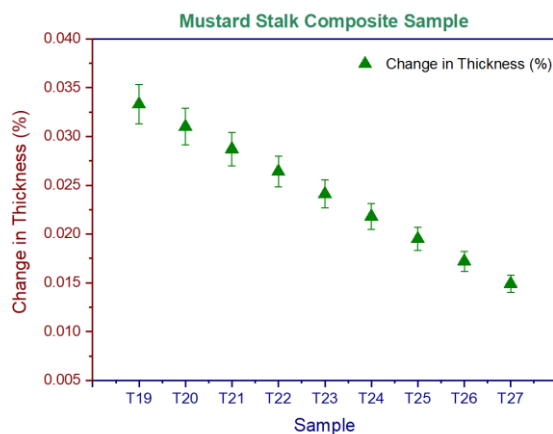


Figure 5.11: Effect of water absorption on swelling for Mustard Stalk composite material

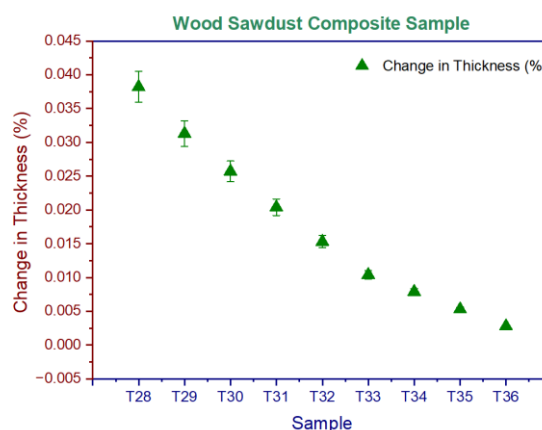


Figure 5.12: Effect of water absorption on swelling for Wood Sawdust composite material

5.4 Results of Weight Density for various Composite

The weight density analysis of various agro-residue composite treatments revealed significant differences across residue types and amounts. For Paddy Straw (T1-T9), as shown in Figure 5.13, the weight density increased gradually with decreasing residue weights, reaching a peak of $0.856 \text{ g}\cdot\text{sec}^2/\text{cm}^2$ at 500 grams (T9). Bagasse (T10-T18), depicted in Figure 5.14, exhibited a similar upward trend, with weight densities ranging from $0.429 \text{ g}\cdot\text{sec}^2/\text{cm}^2$ to $0.709 \text{ g}\cdot\text{sec}^2/\text{cm}^2$. Mustard Stalk (T19-T27), also shown in Figure 5.14, demonstrated moderate increases in weight density, peaking at $0.700 \text{ g}\cdot\text{sec}^2/\text{cm}^2$ at 500 grams (T27). Among the Wood Sawdust samples (T28-T36), shown in Figure 5.15, the weight density was the highest, with values ranging from $0.527 \text{ g}\cdot\text{sec}^2/\text{cm}^2$ to $0.918 \text{ g}\cdot\text{sec}^2/\text{cm}^2$. The T32 sample of Wood Sawdust, containing 600 grams of residue, showed a weight density of $0.733 \text{ g}\cdot\text{sec}^2/\text{cm}^2$, indicating a notable density value despite the higher residue content. This suggests that the T32 composite, with its higher weight, maintains a relatively balanced weight density compared to other samples with lower residue amounts, highlighting the influence of residue type and concentration on the composite's properties.

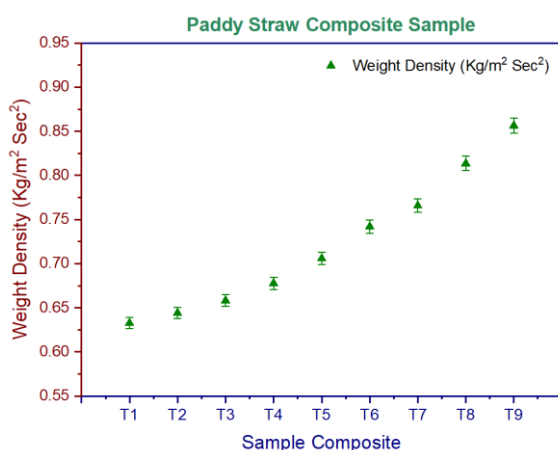


Figure 5.13: Weight density for Paddy Straw composite material

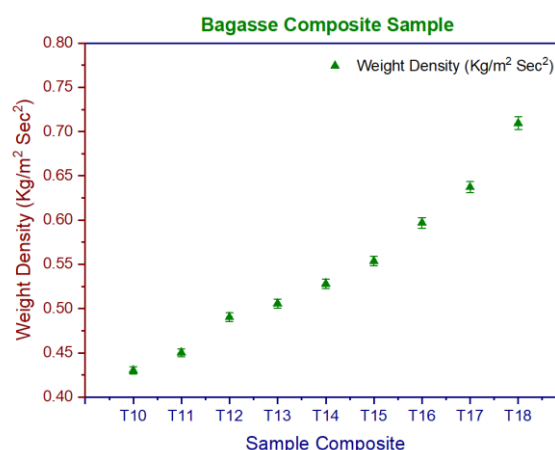


Figure 5.14: Weight density for Bagasse composite material

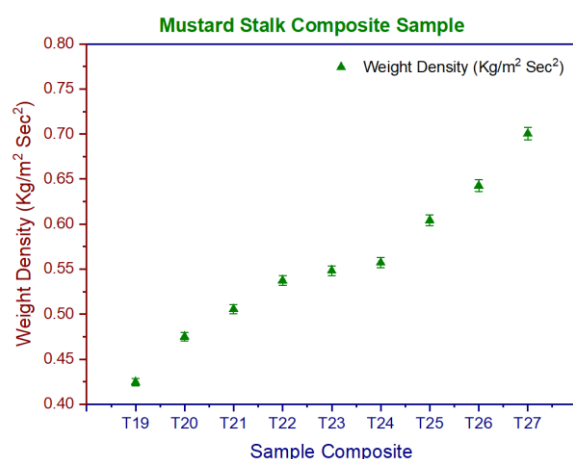


Figure 5.15: Weight density for Mustard Stalk composite material

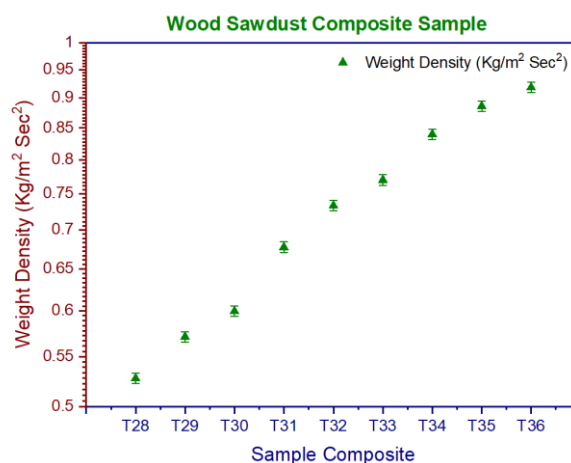


Figure 5.16: Weight density for Wood Sawdust composite material

6. Cost Analysis of Agro-Residue-Based Composite Panels

To evaluate the material feasibility of agro-residue-based composite panels compared to conventional construction materials such as brick masonry, cement concrete, and steel sheet bins, a comprehensive cost analysis was conducted. Each batch developed for the panel fabrication consisted of agricultural residues—including paddy straw, bagasse, mustard stalk, and wood sawdust—in varying quantities ranging from 500 to 700 grams, along with a fixed 100 grams of silica filler and 100 millilitres of a mixture of epoxy resin and hardener. The resin and hardener were combined in a 3:1 ratio for all formulations.

6.1 Material Cost Assumptions

The cost evaluation was based on prevailing conservative market estimates. Agricultural residues were locally sourced and priced at ₹2.00 per kilogram. The silica filler, of industrial grade, was priced at ₹40.00 per kilogram, while the standard-grade epoxy hardener was considered at ₹200.00 per litre. The cost of epoxy resin was not calculated separately, as it was mixed proportionately with the hardener during preparation. For comparative reference, the conventional construction materials were assumed to have the following costs: brick masonry at ₹600.00 per square meter, cement concrete ranging between ₹400.00 and ₹600.00 per unit, and steel sheet bins at ₹85.00 per kilogram (approximately ₹850.00 for a 10-kilogram sheet).

6.2 Composition and Batch-Wise Cost Computation

Batch-wise cost computations were performed based on three primary components: silica, hardener, and agricultural residue. The cost of silica filler was ₹4.00 per 100 grams, while the hardener cost was ₹20.00 per 100 milliliters. The cost of agricultural residue varied according to the quantity used, ranging from ₹1.00 for 500 grams to ₹1.40 for 700 grams. The total material cost per batch was calculated by summing the costs of the silica filler, hardener, and the respective quantity of agricultural residue. Table 10 provides the detailed batch composition and corresponding material costs.

Table 10: Composition Cost Analysis of Agro-Residue Composite Panels

S. No.	Treatment ID	Agro-Residue Type	Residue Weight (g)	Residue Cost (INR)	Silica Cost (INR)	Hardener Cost (INR)	Total Cost (INR)
1	T1	Paddy Straw	700	1.40	4.00	20.00	25.40
2	T2	Paddy Straw	675	1.35	4.00	20.00	25.35
3	T3	Paddy Straw	650	1.30	4.00	20.00	25.30
4	T4	Paddy Straw	625	1.25	4.00	20.00	25.25
5	T5	Paddy Straw	600	1.20	4.00	20.00	25.20

6	T6	Paddy Straw	575	1.15	4.00	20.00	25.15
7	T7	Paddy Straw	550	1.10	4.00	20.00	25.10
8	T8	Paddy Straw	525	1.05	4.00	20.00	25.05
9	T9	Paddy Straw	500	1.00	4.00	20.00	25.00
10	T10	Bagasse	700	1.40	4.00	20.00	25.40
11	T11	Bagasse	675	1.35	4.00	20.00	25.35
12	T12	Bagasse	650	1.30	4.00	20.00	25.30
13	T13	Bagasse	625	1.25	4.00	20.00	25.25
14	T14	Bagasse	600	1.20	4.00	20.00	25.20
15	T15	Bagasse	575	1.15	4.00	20.00	25.15
16	T16	Bagasse	550	1.10	4.00	20.00	25.10
17	T17	Bagasse	525	1.05	4.00	20.00	25.05
18	T18	Bagasse	500	1.00	4.00	20.00	25.00
19	T19	Mustard Stalk	700	1.40	4.00	20.00	25.40
20	T20	Mustard Stalk	675	1.35	4.00	20.00	25.35
21	T21	Mustard Stalk	650	1.30	4.00	20.00	25.30
22	T22	Mustard Stalk	625	1.25	4.00	20.00	25.25
23	T23	Mustard Stalk	600	1.20	4.00	20.00	25.20
24	T24	Mustard Stalk	575	1.15	4.00	20.00	25.15
25	T25	Mustard Stalk	550	1.10	4.00	20.00	25.10
26	T26	Mustard Stalk	525	1.05	4.00	20.00	25.05
27	T27	Mustard Stalk	500	1.00	4.00	20.00	25.00
28	T28	Wood Sawdust	700	1.40	4.00	20.00	25.40
29	T29	Wood Sawdust	675	1.35	4.00	20.00	25.35
30	T30	Wood Sawdust	650	1.30	4.00	20.00	25.30
31	T31	Wood Sawdust	625	1.25	4.00	20.00	25.25
32	T32	Wood Sawdust	600	1.20	4.00	20.00	25.20
33	T33	Wood Sawdust	575	1.15	4.00	20.00	25.15
34	T34	Wood Sawdust	550	1.10	4.00	20.00	25.10
35	T35	Wood Sawdust	525	1.05	4.00	20.00	25.05
36	T36	Wood Sawdust	500	1.00	4.00	20.00	25.00

6.3 Comparison with Conventional Construction Materials

To evaluate the economic viability of agro-residue-based composites, a comparison was made with traditional materials based on several key factors, including unit cost, durability, eco-friendliness, weight, and overall performance. The detailed comparison is presented in Table 11, which illustrates the differences between the agro-residue composite panels and conventional materials across these parameters.

Table 11: Comparison of Agro-Residue Composite Panels with Conventional Materials

S. No.	Material Type	Approximate Cost per Unit (INR)	Durability	Eco-Friendliness	Weight	Remarks
1	Brick Masonry	₹600/m ²	High	Low	Very High	Labor-intensive, non-biodegradable
2	Cement Concrete	₹400–₹600	High	Low	High	High CO ₂ footprint
3	Steel Sheet Bin	₹850 (10 kg)	Very High	Low	High	Expensive, recyclable but energy-intensive
4	Agro-Composite (T32)	₹25.20	Moderate–High	High	Light	Cost-effective, biodegradable, rural-suitable

6.4 Economic and Technical Evaluation

From an economic standpoint, sample T32 (wood sawdust, 600 g) emerged as the most efficient formulation, combining moderate residue weight with a low total material cost of ₹25.20 per batch. Technically, T32 demonstrated acceptable physical properties, including weight density, water absorption, and thickness swelling characteristics, making it suitable for practical applications.

In terms of cost savings, the agro-residue composites significantly reduced material costs—by more than 90% compared to brick masonry and steel bins. Environmentally, utilizing wood sawdust diverted waste from landfill streams, reduced the carbon footprint, and aligned with circular economy principles. Additionally, the lightweight nature of T32 composites enables modular construction and easy transportation, which is especially advantageous for rural grain storage systems.

6.5 Justification for T32 as the Most Cost-Effective Treatment

The T32 sample, fabricated with 600 grams of wood sawdust, 100 grams of silica filler, and 100 milliliters of epoxy hardener, proved to be the most cost-effective and technically feasible choice. Several factors contributed to its selection:

- It achieved a balance between mechanical strength and minimal use of costly resin and hardener.
- The residue cost was only ₹1.20, contributing approximately 5% of the total material cost.
- Since silica and hardener costs remained constant across treatments, optimizing the residue content reduced the overall material cost.
- The total material cost of ₹25.20 per batch was significantly lower than traditional construction materials.
- Moreover, wood sawdust is abundant, inexpensive, and lightweight, enhancing handling and field installation efficiencies.

Thus, T32 provides an optimal solution that combines cost-effectiveness, environmental sustainability, and technical performance, making it highly suitable for developing low-cost, eco-friendly construction materials targeted at rural and resource-constrained regions.

7. Uncertainty Assessment and Correlation Development for Composite Material Properties

In this section, the uncertainties related to key experimental measurements including weight, dimensions, water absorption, and density are systematically evaluated to ensure the reliability of the results. Measurement uncertainties are quantified using the Kline and McClintock method. Furthermore, empirical correlation equations

are developed to describe the relationships between critical physical properties, such as the density of the fabricated agro-residue composite materials. This approach enhances the accuracy and predictive capability of the study's findings.

7.1 Uncertainty Analysis

In experimental research, errors are inevitable, even with careful precautions. To ensure the validity of experimental results, it is essential to evaluate and identify the primary sources of error that may affect the measurements. During an experiment, the recorded data often deviates from the actual values due to various unaccounted factors inherent in the experimental setup. This deviation, referred to as uncertainty, must be quantified to assess the reliability of the data.

To measure and account for uncertainty, a method such as the Kline and McClintock [45]-[47] approach is commonly used. This widely recognized methodology allows for the estimation of uncertainties associated with different components and devices, as summarized in Table 12. The general procedure for evaluating uncertainty is as follows:

For a parameter y determined by several measured quantities x_1, x_2, \dots, x_n , the equation to estimate the uncertainty in y is:

$$y = y(x_1, x_2, x_3, \dots, x_n) \quad \dots (7.1)$$

The uncertainty in y , denoted as δy , is determined by the formula:

$$\left[\left(\frac{\partial y}{\partial x_1} \delta x_1 \right)^2 + \left(\frac{\partial y}{\partial x_2} \delta x_2 \right)^2 + \dots + \left(\frac{\partial y}{\partial x_n} \delta x_n \right)^2 \right]^{1/2} \quad \dots (7.2)$$

Where $\delta x_1, \delta x_2, \dots, \delta x_n$ represent the potential errors in the measurements of the variables x_1, x_2, \dots, x_n . Here, δy represents the absolute uncertainty, and the relative uncertainty is expressed as $\frac{\delta y}{y}$. This approach ensures that all potential sources of error are considered and that the overall uncertainty in the experimental results is properly quantified, leading to more accurate and reliable conclusions for the development and optimization of grain storage composites using crop residues.

Table 12: Uncertainty in various measuring parts and devices

Sl. No.	Operations	Instrument	Least Count	Error
1	Weighing Composite Sample	Digital Balance	0.001 g	± 0.01 g
2	Composite Sample Size	Caliper Scale	0.01 mm	± 0.05 mm
3	For Homogenization	Mixing Tray	N/A	$\pm 1\%$ variation
4	For Casting Composite Material	Mould	N/A	$\pm 2\%$ dimensional variation
5	For Pressing	Screw Jack Pressure	0.1 N	± 0.5 N
6	Water Absorption Measurement	Digital Balance, Water Bath	0.001 g (Balance), N/A (Water Bath)	± 0.01 g (Balance), $\pm 1\%$ (Water Bath)
7	Sieve Analysis	Sieve Shaker, Sieve Set, Digital Balance	0.01 g (Balance), N/A (Sieve Set)	± 0.05 g (Balance), $\pm 2\%$ (Sieve)

Table 13: Uncertainty in Various Parameter

S. No.	Parameter	Uncertainty (%)
1	Weighing Composite Sample	$\pm 0.1\%$
2	Composite Sample Size	$\pm 0.5\%$
3	For Homogenization	$\pm 1\%$

4	For Casting Composite Material	$\pm 2\%$
5	For Pressing	$\pm 0.5\%$
6	Water Absorption Measurement	$\pm 0.1\%$ (Balance), $\pm 1\%$ (Water Bath)
7	Sieve Analysis	$\pm 0.5\%$ (Balance), $\pm 2\%$ (Sieve)

7.2 Correlation

The average weight density for Paddy Straw (A) has been found to be correlated with the Residue-Epoxy Ratio (RER) through the following regression equation:

$$A = 0.8564 - 1.087 \log_{10} (\text{RER}) + 1.319 \log_{10} (\text{RER})^2 - 0.040 \log_{10} (\text{RER})^3 \quad \dots (7.1)$$

Where A represents the weight density in units of $\text{g/sec}^2 \cdot \text{cm}^2$ for Paddy Straw. Similarly, the regression equation for weight density (B) for Bagasse is given by:

$$B = 0.7073 - 1.705 \log_{10} (\text{RER}) + 5.117 \log_{10} (\text{RER})^2 - 6.949 \log_{10} (\text{RER})^3 \quad \dots (7.2)$$

Where B represents the weight density in units of $\text{g/sec}^2 \cdot \text{cm}^2$ for Bagasse. For Mustard Stalk, the weight density (C) is described by the following regression equation:

$$C = 0.7022 - 1.675 \log_{10} (\text{RER}) + 6.397 \log_{10} (\text{RER})^2 - 10.60 \log_{10} (\text{RER})^3 \quad \dots (7.3)$$

Where C denotes the weight density in units of $\text{g/sec}^2 \cdot \text{cm}^2$ for Mustard Stalk. Lastly, the regression equation for Wood Sawdust is given as:

$$D = 0.9197 - 0.7168 \log_{10} (\text{RER}) - 3.309 \log_{10} (\text{RER})^2 + 6.438 \log_{10} (\text{RER})^3 \quad \dots (7.4)$$

Where D represents the weight density in units of $\text{g/sec}^2 \cdot \text{cm}^2$ for Wood Sawdust.

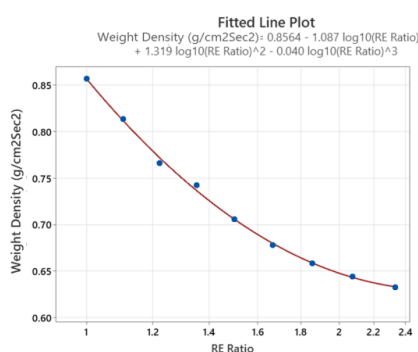


Figure 5.17: Fitted line plot for Paddy Straw composite material

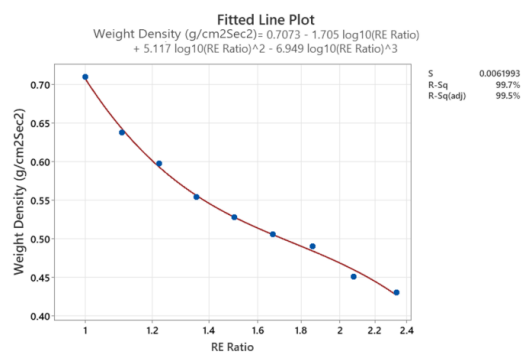


Figure 5.18: Fitted line plot for Bagasse composite material

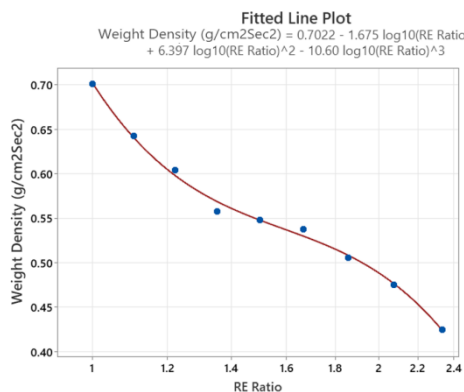


Figure 5.19: Fitted line plot for Mustard Stalk composite material

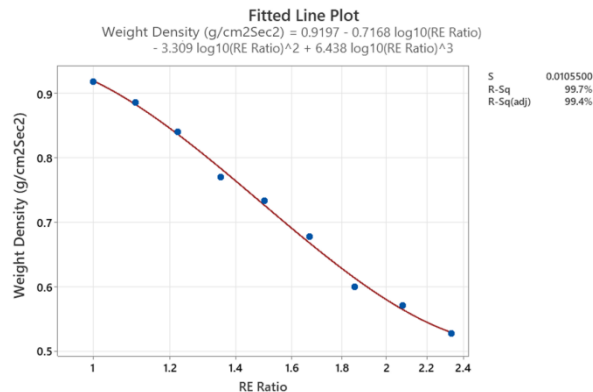


Figure 5.20: Fitted line plot for Wood Sawdust composite material

The Residue-Epoxy Ratio (RER), varying between 2.3333 and 1, was correlated with the weight density of the fabricated agro-residue composite materials. The generated correlation curves demonstrated a strong fit with the experimental data, as indicated by the high R-squared (R^2) and adjusted R-squared (Adj- R^2) values. Specifically, the correlation for paddy straw composites achieved an R^2 of 99.8% and an Adj- R^2 of 99.7%, as depicted in Figure 5.17. Similarly, for bagasse composites, the R^2 and Adj- R^2 values were 99.7% and 99.5%, respectively (Figure 5.18); for mustard stalk composites, they were 99.6% and 99.3% (Figure 5.19); and for wood sawdust composites, they were 99.7% and 99.4% (Figure 5.20).

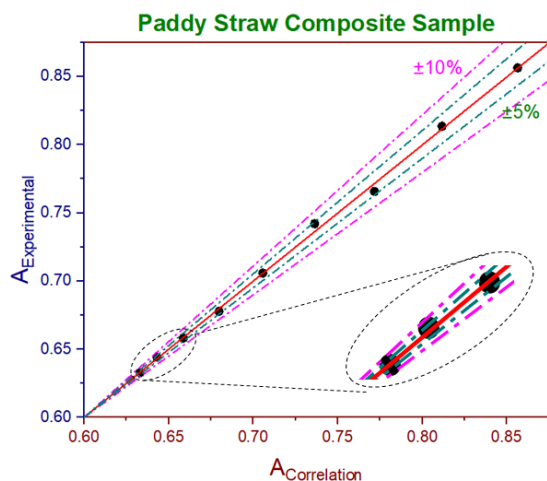


Figure 5.21: A comparison between experimental Weight density and correlation weight density

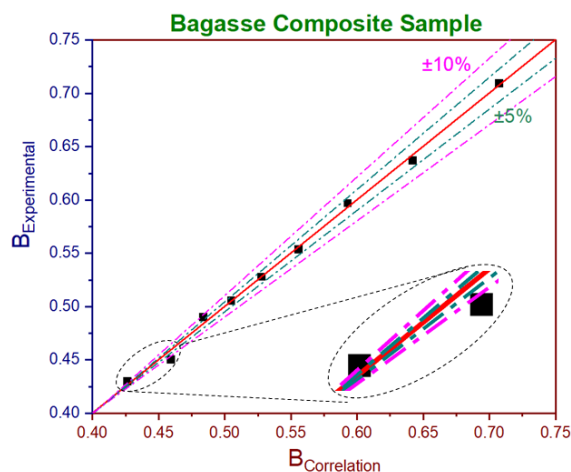


Figure 5.22: A comparison between experimental Weight density and correlation weight density

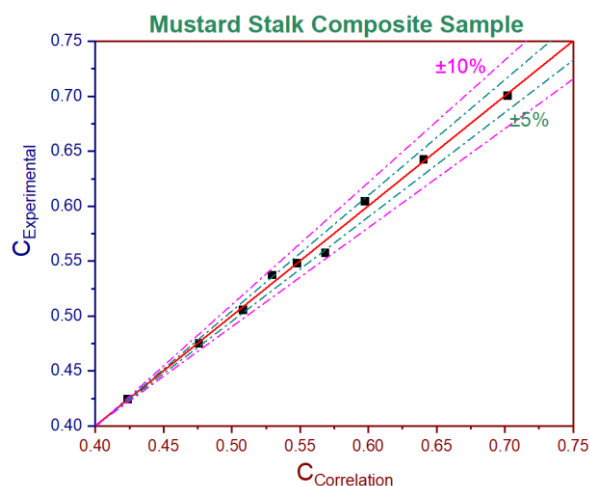


Figure 5.23: A comparison between experimental Weight density and correlation weight density

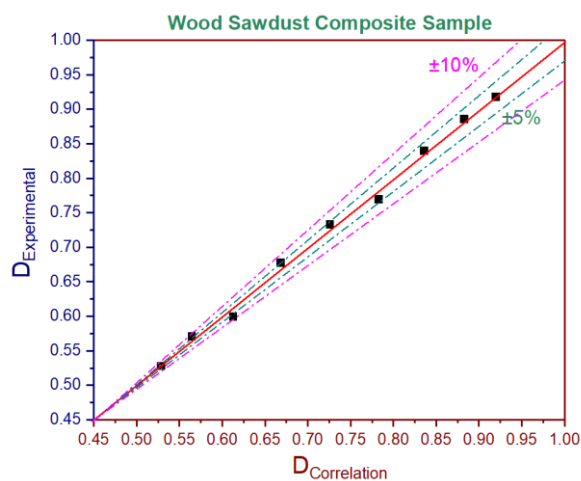


Figure 5.24: A comparison between experimental Weight density and correlation weight density

Furthermore, Figures 5.21 to 5.24 illustrate a direct comparison between the predicted weight densities obtained from the correlation equations and the actual experimental results. A substantial majority of the experimental data points are located within a $\pm 10\%$ uncertainty band, confirming a high level of agreement between the theoretical predictions and experimental observations. This close alignment demonstrates the robustness and predictive capability of the developed correlation models.

However, it is noteworthy that two data points corresponding to the bagasse-based composites fell outside the $\pm 10\%$ uncertainty range, indicating minor deviations. Despite these outliers, the overall model performance remains highly reliable, providing consistent and accurate predictions for the weight density of agro-residue composite panels across the investigated RER range.

8. Conclusion: Impact of Crop Residue-Based Composites on Sustainable Agriculture

This study highlights the potential of agro-based composite materials, particularly those fabricated with 600 grams of wood sawdust, 100 grams of silica filler, and 100 millilitres of epoxy hardener, for use in sustainable grain storage. By utilizing agricultural waste, these composites present an eco-friendly and cost-effective alternative to traditional materials, particularly in resource-limited regions. Key findings from the study, including water absorption and density tests, reveal valuable insights into the performance of these materials.

8.1 Key Findings for T32 Composite Sample:

(i) Sieve Analysis:

- The sieve analysis showed appropriate particle size distribution of the wood sawdust, crucial for a homogeneous mix with silica and epoxy.
- The granularity of the agro-residue was suitable, ensuring optimal structural integrity and performance in grain storage applications.

(ii) Water Absorption:

- The water absorption test revealed favourable results, with the composites demonstrating a relatively low water absorption rate.
- This indicates that the composites are effective at resisting moisture penetration, which is essential for long-term grain storage.

(iii) Shrinkage and Swelling:

- Shrinkage and swelling tests indicated minimal dimensional changes under varying humidity conditions.
- This suggests that the composites offer excellent dimensional stability, making them suitable for environments with fluctuating moisture levels.

(iv) Weight Density:

- The weight density of the composites was measured, with the T32 sample (wood sawdust, silica, and epoxy) achieving a balanced density.
- This density is crucial for ensuring the structural integrity of the panels while providing effective insulation for grain storage.

(v) Cost Analysis:

- Cost computations for the batch fabrication of the composites showed a competitive material cost, especially considering the potential reduction in post-harvest losses.
- Future studies can explore further optimization to reduce material costs and improve the composites' economic viability.

(vi) Comparison with Conventional Materials:

- When compared to traditional grain storage materials, the agro-residue composite panels exhibited comparable or superior performance in terms of moisture resistance and dimensional stability.
- The use of agricultural waste also offers environmental benefits, making these composites a sustainable alternative, especially for regions with limited resources.

8.2 Future Research Directions

The results of this study point to the feasibility of scaling up the production of these agro-based composites for broader application. Future research should focus on optimizing the formulation of these composites, exploring their long-term performance under real-world storage conditions, and assessing their durability over extended use. Additionally, further investigation into the impact of environmental factors such as temperature and humidity on the material properties will be crucial for ensuring their practical viability for grain storage in varying climates.

References

- [1] Singh, M. Gupta, and N. Verma, "Life cycle assessment of grain storage materials in rural India," *Environ. Eng. Res.*, vol. 25, no. 4, pp. 569–578, 2020.
- [2] R. Kumar, V. Sharma, and P. Mishra, "Valorization of agricultural residues for sustainable construction materials," *J. Cleaner Prod.*, vol. 293, p. 125866, 2021.
- [3] V. R. Sashidhar *et al.*, "Physico-chemical aspects of grain deterioration," *J. Food Sci. Technol.*, vol. 29, no. 1, pp. 15–22, 1992.
- [4] Kartikeyan *et al.*, "Post-harvest storage losses in food grains," *Indian J. Agric. Sci.*, vol. 79, no. 2, pp. 121–125, 2009.
- [5] M. Greeley, "Storage in Indian agriculture: A farm-level perspective," *Econ. Polit. Weekly*, vol. 13, no. 22, pp. A60–A68, 1978. D. Kumar and P. Kalita, "Reducing postharvest losses during storage of grain crops," *Food Secur.*, vol. 9, no. 5, pp. 835–848, 2017.
- [6] A. Manandhar *et al.*, "Traditional grain storage practices in Nepal," *J. Food Sci. Agric.*, vol. 95, no. 3, pp. 493–500, 2018.
- [7] V. Channal *et al.*, "Survey of traditional storage structures," *Agric. Eng. Today*, vol. 28, no. 3, pp. 1–6, 2004.
- [8] J. A. Osunade, "Design of reinforced concrete silos," *J. Agric. Eng. Res.*, vol. 48, no. 3, pp. 173–186, 1991.
- [9] K. John, "Wooden silos: Benefits and limitations," *Indian For.*, vol. 121, no. 7, pp. 612–616, 1995.
- [10] Y. Mijinyawa *et al.*, "Termite mound clay in silo construction," *Agric. Mech. Asia Afr. Latin Am.*, vol. 38, no. 1, pp. 43–48, 2007.
- [11] M. Omobowale *et al.*, "Performance of TMC, GS and RC silos," *J. Stored Prod. Res.*, vol. 61, pp. 1–7, 2015.
- [12] A. Nganga *et al.*, "Hermetic bags for maize storage," *Food Chain*, vol. 6, no. 3, pp. 253–261, 2016.
- [13] G. Kuraloviyana *et al.*, "Development of hermetic millet bins," *ICRISAT Tech. Bull.*, no. 43, pp. 1–8, 2020.
- [14] K. Lakshmi *et al.*, "Household use of hermetic storage," *Int. J. Agric. Sci.*, vol. 10, no. 2, pp. 158–164, 2020.
- [15] R. B. Mathur, "Use of agro-residues in construction," *J. Mater. Environ. Sci.*, vol. 8, no. 5, pp. 1455–1462, 2006.
- [16] P. Wambua, J. Ivens, and I. Verpoest, "Natural fibres: Applications and performance," *Compos. Sci. Technol.*, vol. 63, pp. 1259–1274, 2003.
- [17] A. Perminov *et al.*, "Effect of nano-silica on epoxy," *Polym. Compos.*, vol. 23, no. 4, pp. 510–519, 2002.
- [18] R. Ou, R. Xie, and Q. Zhou, "Mechanical properties of silica-filled composites," *Mater. Lett.*, vol. 36, pp. 242–246, 1998.
- [19] K. Wang, M. Li, and Y. Zhang, "Calcium carbonate in epoxy composites," *Polym. Eng. Sci.*, vol. 42, pp. 162–172, 2002.
- [20] J. Osarenmwinda *et al.*, "Prediction models for agro-composites," *Niger. J. Technol.*, vol. 29, no. 2, pp. 109–115, 2010.
- [21] S. Junjun, Y. Sun, and M. Zhao, "Starch-reinforced rice straw composites," *BioResources*, vol. 7, no. 4, pp. 5324–5335, 2012.
- [22] Y. Liu, B. Wang, and X. He, "Water-resistant composites from rice straw," *Constr. Build. Mater.*, vol. 33, pp. 206–210, 2012.
- [23] Verma *et al.*, "Bamboo-epoxy fiber composites," *Adv. Compos. Lett.*, vol. 23, pp. 71–76, 2014.
- [24] H. Manji, P. Naik, and R. Kumar, "Mechanical behavior of rice straw composites," *Int. J. Appl. Eng. Res.*, vol. 9, no. 12, pp. 1879–1886, 2014.
- [25] N. Dsouza, A. Jain, and R. Prasad, "Bio-composites for yak saddles," *J. Nat. Fibers*, vol. 13, no. 2, pp. 180–190, 2016.

- [26] B. A. Adejumo, "Design of low-cost metal silo," *Int. J. Agric. Innov.*, vol. 1, no. 2, pp. 45–50, 2013.
- [27] R. K. Bhardwaj, "Evaluation of storage bins under humid conditions," *Indian Agric. Res. J.*, vol. 48, no. 4, pp. 310–314, 2014.
- [28] R. Verma and P. Goel, "Mechanical and moisture behavior of natural fiber reinforced composites using silica filler," *Mater. Res. Express*, vol. 6, no. 10, p. 105309, 2019.
- [29] Bureau of Indian Standards (BIS), *IS: 2380 – Methods of Test for Wood Particle Boards and Boards from Other Lignocellulosic Materials*, Parts 3 and 16, New Delhi, India, 1977.
- [30] Thakur and S. Raj, "Sustainable hybrid composites using agricultural residues for low-cost housing," *Constr. Build. Mater.*, vol. 230, p. 116933, 2019.
- [31] M. Jain, R. Bansal, and H. Agarwal, "Biocomposites for packaging and storage applications: Current trends and future prospects," *Polym. Environ.*, vol. 29, no. 3, pp. 657–672, 2021.
- [32] J. P. Pascault, H. Sautereau, J. Verdu, and R. J. J. Williams, *Thermosetting Polymers*. Marcel Dekker, 2002.
- [33] Huntsman Advanced Materials, "Technical Data Sheet: Araldite® CY 230," Huntsman Corporation, 2010.
- [34] H. Bacon, "Electrical insulation properties of epoxy resins," *IEEE Trans. Electr. Insul.*, vol. 20, no. 5, pp. 879–885, Oct. 1985.
- [35] P. Morgan, *Carbon Fibers and Their Composites*. CRC Press, 2005.
- [36] S. Singh, "Curing kinetics and mechanical characterization of epoxy resin systems," *J. Polym. Eng.*, vol. 32, no. 4, pp. 203–211, 2012.
- [37] J. Zhang, G. Z. Zhang, and Y. C. Chan, "Effect of nano-silica size on the mechanical properties of epoxy composites," *Journal of Applied Polymer Science*, vol. 111, no. 5, pp. 2462–2468, 2009.
- [38] J. D'Souza, "Nano Silica Reinforced Epoxy Composites for Enhanced Wear and Friction Performance," *International Journal of Engineering Science and Technology*, vol. 8, no. 2, pp. 53–60, 2016.
- [39] M. S. Cao and Y. Q. Du, *Silica Nanoparticles: Structure, Properties, and Applications*, Elsevier, 2021.
- [40] A. Singh, R. Kumar, and A. Sharma, "Effect of bio-waste fillers on the mechanical and thermal properties of epoxy-based composites," *Journal of Composite Materials*, vol. 46, no. 12, pp. 1513–1521, 2012.
- [41] B. C. Agrawal, R. N. Singh, and J. K. Sharma, "Mechanical properties of unsaturated polyester resin reinforced with natural fibers," *Journal of Materials Science*, vol. 25, no. 9, pp. 3950–3956, 1990.
- [42] ASTM D5229/D5229M-20, *Standard Test Method for Moisture Absorption Properties and Equilibrium Conditioning of Polymer Matrix Composite Materials*, ASTM International, West Conshohocken, PA, 2020.
- [43] Montgomery, D.C., *Design and Analysis of Experiments*, 9th ed., Wiley, 2017. This textbook provides a detailed explanation of the ANOVA methodology, including the formulas for mean squares and how they are used in hypothesis testing.
- [44] ASTM E11, "Standard Specification for Woven Wire Test Sieve Cloth and Test Sieves," ASTM International, 2016.
- [45] R. J. Moffat, "Describing the uncertainties in experimental results," *Experimental thermal and fluid science*, vol. 1, no. 1, pp. 3–17, 1988.
- [46] R. Moffat, "Contributions to the theory of single-sample uncertainty analysis," 1982.
- [47] S. J. Kline, "Describing uncertainties in single-sample experiments," *Mech. Eng.*, vol. 75, pp. 3–8, 1963.